# Dynamic FOV Tracking Receiver for Dense Optical Networks

I. Abdalla,* M.B. Rahaim,† T.D.C. Little,*
*Electrical and Computer Engineering Department, Boston University, Boston, MA USA
†Engineering Department, University of Massachusetts at Boston, Boston, MA USA
*imanha@bu.edu, michael.rahaim@umb.edu, tdcl@bu.edu*

***Abstract*—Dense networks are characterized by the prevalence of wireless access points (APs) in close proximity to a population of user devices on a similar scale. This is in contrast with a legacy model of a single AP serving many devices. By increasing AP density, the aggregate data consumption of the system can be dramatically increased.**

**In this paper we consider dense deployment of directional optical access points. In particular, we analyze how a user device can select and track a transmitter then adapt its field of view (FOV) to achieve the best signal quality within the array of APs. Using a geometric model for an indoor space and a reference optical channel model, we formulate an optimization problem with a goal of optimizing FOV for maximum signal to noise ratio (SNR). The results, applied as a proposed dynamic FOV technique with receiver tracking capability, show an average SNR increase of up to 40% when compared to a fixed receiver associated with a user device with dynamic translational/rotational motion. These results motivate the adoption of dynamic pointing and adaptive FOV at the receiver in order to realize improved performance for mobile devices in a dense optical wireless network.**

***Index Terms*—LiFi, multi-cell lighting, visible light communications (VLC), optical wireless communications (OWC), handover, dense networks**

## I. Introduction

Wireless local area networks (WLANs) and cellular telephony have both evolved substantially in the last two decades. WLANs rapidly emerged to support laptops in an office setting whereas cellular services have proliferated and adopted small cells as a means to accommodate an increase in user density. The onset of multi-radio smartphones with WiFi along with the low cost and availability of low power (Zigbee, Bluetooth, and WiFi) microcontroller hardware has greatly boosted the density of wireless devices - particularly in the indoor environment. The response in both communities is to increase the capacity and density of access points (APs); however, managing interference from adjacent devices continues to be critical especially as the AP placement density increases. Many researchers expect that the use of optical media in the IR or visible spectrum can exploit directionality and the large optical bandwidth potential to both increase link capacity and mitigate inter-cell (inter-AP) interference.

With the directional property of light we can expect to control the channel either at the transmitter [1] or the receiver, or both. In this paper we focus on control at the receiver. Based on prior analysis [2], we have shown how FOV plays an important role in improving signal quality by removing unnecessary incident noise on a receiver photodetector. Similarly, the impact of orientation of a receiver on signal quality has been analyzed and validated in practical OWC systems [3].

Based on the advantages of FOV and orientation control [2], [4], we seek to jointly control the dynamics of these degrees of freedom, and to optimize signal delivery under device mobility and orientation. The proposed solution involves an adaptive technique that minimizes the frequency of AP handovers to realize overall performance gain.

Related work includes efforts for localization and receiver tracking in optical wireless visible light communications such as references [5]–[7]; however, there is scarcity of work on tracking of transmitters for the indoor AP problem which has wide angle deviations unlike, for example, building-to-building free space optics (FSO). In reference [8], the authors propose an algorithm for tracking by discretizing the receiver azimuth angle domain and subsequently performing an exhaustive search on this space. In contrast, our work relies on closed-form solutions which are faster and more accurate.

The main contributions of this work are:

- Development of an optimized adaptive technique for variable device location and orientation.
- Development of a novel receiver FOV dynamic optimization technique (where the FOV is varied by an adjustable opening without any lens/optics) to realize best performance in terms of reduced handovers and increased average SNR.
- Analysis and simulation demonstrating performance gains over static cases with up to 40% increase in average SNR.

The remainder of the paper is organized as follows: Section II describes our system model. Section III explores our proposed dynamic FOV (D-FOV) Tracking receiver. Section IV discusses our simulation results. Section V concludes the paper.

## II. System Model

Here we describe the channel model for an OWC receiver in the context of an overhead access point (AP). This includes the geometry characterizing the AP, the mobile user device, and its field of view (FOV).

This work was supported in part by the Engineering Research Centers Program of the National Science Foundation under NSF Cooperative Agreement No. EEC-0812056 and by NSF No. CNS-1617924.

I. Abdalla, M. B. Rahaim and T. D. C. Little, "Dynamic FOV Tracking Receiver for Dense Optical Wireless Networks," 2019 IEEE Global Communications Conference (GLOBECOM), Waikoloa, HI, USA, 2019, pp. 1-6, doi: 10.1109/GLOBECOM38437.2019.9014277.

In our experiments we use commercial LED-based CREE luminaires which are rectangular in form. In our simulated environment, these are modeled as a grid of $w \times n$ point sources (or elements). The element Line of Sight (LOS) optical channel DC gain [9], the gain from a transmitting element to receiver, is defined as:

$$H^{ji}_{DC,e}(\phi_{ji}, \psi_{ji}, d_{ji}) = \frac{P^{(ji)}_{r,e}}{P^{(ji)}_{t,e}} = \frac{G_T(\phi_{ji})G_R(\psi_{ji})}{d^2_{ji}}, \quad (1)$$

where $P^{(ji)}_{t,e}$ and $P^{(ji)}_{r,e}$ are the optical power transmitted and received from the $i$-th element within transmitter $j$, respectively. $\phi_{ji}$ is the emission angle, $\psi_{ji}$ is the acceptance angle, and $d_{ji}$ is the distance between the receiver and the $i$-th element, as shown in Fig. 1. All the parameters defined with subscript/superscript $ji$ describe the point source element $i$ within source $j$. The transmitter gain (i.e., $G_T$) and the receiver gain (i.e., $G_R$) are defined as:

$$G_T(\phi) = \frac{m+1}{2\pi}\cos^m(\phi) \quad (2)$$

and

$$G_R(\psi) = A\cos(\psi)1\{\psi < \chi\} \quad (3)$$

respectively. We consider a Lambertian emission with order $m$ and model a photodetector with area $A$ and no filter or optical lens. $\chi$ is the receiver's FOV and $1\{.\}$ represents the indicator function.

We consider signal transmission via Intensity Modulation with Direct Detection (IM/DD). Substituting in Eq. 1, the optical power received from element $i$ is evaluated as:

$$P^{(ji)}_{r,e} = \frac{P^{(ji)}_{t,e}(m+1)A\cos^m\phi_{ji}cos\psi_{ji}}{2\pi d^2_{ji}}1\{\psi_{ji} < \chi\} \quad (4)$$

where $P^{(ji)}_{t,e} = P^{(j)}_t\alpha_{ji}$. We define $P^{(j)}_t$ as the optical power transmitted from source $j$; therefore, $\sum_i \alpha_{ji} = 1$. In this paper we consider $\alpha_{ji} = \frac{1}{wn}\forall i$ to normalize the transmitter's power over all the elements that it contains.

The transmitter LOS channel gain which sums over all the elements $i$ within the transmitter $j$ is

$$H^j_{DC} = \sum_{i=1}^{wn}\alpha_{ji}H^{ji}_{DC,e} \quad (5)$$

The total received optical power from the $j$-th transmitter can be evaluated using

$$P^{(j)}_r = \sum_{i=1}^{wn}P^{(ji)}_{r,e} \quad (6)$$

## III. Dynamic FOV Tracking at the Receiver

We have established the benefits of optimizing FOV for a static link in prior work [3]. Similarly, adjusting the receiver's orientation in response to the AP's relative location can improve performance. In the following, we propose and explore how dynamic receiver FOV and orientation can be used to track the visibility of overhead APs under device movement

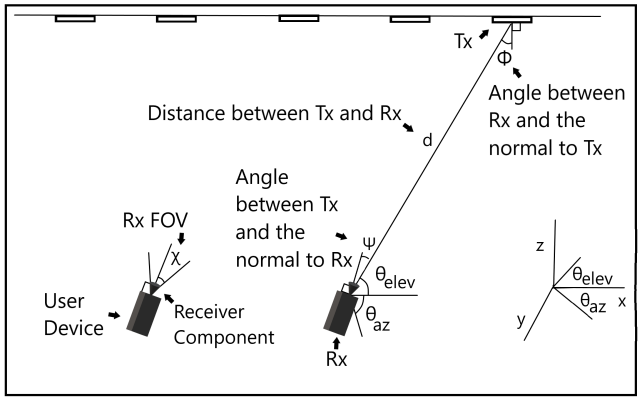


Fig. 1: Device Orientation

including orientation with respect to the AP. We also seek as part of this analysis to realize a minimal number of handovers under these dynamics while sustaining some minimum signal quality constraint defined as threshold $\beta$.

Such a receiver has many benefits. Firstly, due to the ability to tune FOV, decreasing the FOV and mitigating the presence of unnecessary noise increases SNR. Secondly, the control of its own orientation allows the receiver to avoid blackout conditions due to inconvenient angles or occlusions; although, occlusions are not specifically addressed here.

We anticipate an additional advantage in that a receiver can be initialized with knowledge of the availability of overhead APs as a basis. From this basis, the receiver can start with a map of available resources that can be exploited in planning the subsequent traversal of the APs under mobility. This frees-up the system (the APs) from the responsibility of tracking mobile users – i.e,. Mobile Assisted Handover, where the mobile users manage the tracking of the APs.

### A. Pointing Analysis

From Eq. (4), we deduce that a receiver can maintain best signal quality if it realizes an angle with respect to the source of $\psi$, keeping it at 0 for best signal level. This is clearly established based on the cosine function for which a peak of 1 is achieved at angle $0^\circ$. We assume the receiver knows the fixed location of the APs and knows its position relative to the APs. We then use our mathematical model to identify the best elevation and azimuth angles that allow the receiver to always position with $\psi = 0$ with respect to the center of the tracked source. These angles, represented in Fig. 1, are geometrically deduced as follows:

$$\theta_{elev} = \tan^{-1}\left(\frac{h}{\sqrt{(x_r - x_t)^2 + (y_r - y_t)^2}}\right) \quad (7)$$

$$\theta_{az} = \tan^{-1}\left(\frac{y_t - y_r}{x_t - x_r}\right) \quad (8)$$

where $h$ is the vertical height between the transmitter and the receiver. $(x_t, y_t)$ and $(x_r, y_r)$ are the x, y coordinates of the transmitter's center and the receiver, respectively.

The receiver finds the closest transmitter to its position within its range of motion (in our simulation we assume that

the receiver has a full range of motion) and locks on to it, changing its FOV dynamically (explained more in III-B) so that it can deliver the highest SNR achievable per the tracked transmitter.

The condition for which the receiver decides to stop tracking one transmitter and lock on to another depends on the configuration of the overall system (room size, AP placement, handover protocol, receiver range of motion, etc.). Under a designed scenario, handover can be based on an SNR threshold constraint, or just following the maximum SNR envelope, which isn't necessarily the best option for reducing number of handovers. One might also add a hysteresis margin to avoid ping-pong effects (i.e., $SNR_1 < Threshold1$, and $SNR_2 - SNR_1 > Threshold2$). We use the SNR threshold $\beta$ as the transition criterion. Once the receiver meets this condition, it initiates pointing and tracking of a new transmitter and subsequent optimization of FOV for the new source.

### *B. Acquisition Analysis*

As for the dynamic FOV model, once the pointing phase decides on the best transmitter to track and the angles $\theta_{elev}$ and $\theta_{az}$, the following model is used to get the FOV that achieves the highest SNR from the tracked transmitter.

Our simulated environment is modelled after the system that we developed [10]. SNR for an On-Off Keying (OOK) modulated signal can be defined as:

$$SNR = \frac{(RP_r)^2}{\sigma_a^2} \tag{9}$$

where $R$ is the receiver responsivity [A/W], $RP_r$ is the current generated at the receiver due to the incident optical power from the associated transmitter and $\sigma_a^2$ is the noise current variance.

For a shot-noise-dominated system, the noise variance $\sigma_a^2$ is modeled as follows [11]: Shot noise is caused by both dark current noise and quantum noise. Dark current noise $\overline{i_d^2}$ is caused by the current flowing in the photodiode independent of the optical signal. $\overline{i_d^2} = 2qI_dB$ where $q$ is the electron charge, $I_d$ is the dark current and $B$ is the receiver bandwidth. Meanwhile, quantum noise $\overline{i_q^2}$ is due to the discrete nature of the photodetection process. $\overline{i_q^2} = 2qRP_nB$ where $P_n$ [W] is the optical power incident on the photodiode. $\overline{i_d^2}$ and $\overline{i_q^2}$ have [$A^2$] units. The noise current variance is

$$\sigma_a^2 = \overline{i_d^2} + \overline{i_q^2} \tag{10}$$

We define the Signal to Noise Ratio (SNR) for transmitter $j$, the transmitter to be tracked, as

$$SNR_j(\chi) = \frac{(RP_t^{(j)}H_{DC}^j)^2}{\sigma_a^2} \tag{11}$$

Note that $P_r^{(j)} = P_t^{(j)}H_{DC}^{(j)}$. We square the sum of the received current of the OOK signals assuming all signal components are synchronized.

$$P_n(\chi) = \sum_j P_{txDC}H_{DC}^j \tag{12}$$

As for $P_n$ we use Eq. (12), where $P_{txDC}$ is the transmitted DC power that contributes to noise. $P_n$ and $P_{txDC}$ are defined in the optical domain. We measure $P_{txDC}$ in the lab to provide credible parameters for the simulation.

In the noise formula, by changing the FOV $\chi$, we are able to count how many elements are included within the FOV to calculate the total optical DC power received at the detector that contributes to shot noise. In this calculation we do not study non-LOS, considering these signals to be negligible on the calculation [12].

On adapting the receiver's FOV, the signal power (Eq. 11) changes as well as the noise DC power (Eq. 12). Hence, to study this effect we form the following optimization problem

$$\begin{aligned} \max_{\chi} \quad & \mathsf{SNR_j}(\chi) \\ \text{s.t.} \quad & 0 \le \chi \le \chi_{\max} \end{aligned}$$

We define $\chi_{max}$ as the maximum FOV that can cover all the sources in the room when the receiver is flat and facing the lights. $\chi_{max}$ can be $90^\circ$ for an unknown space or it can be deduced geometrically for any known room setting depending on the physical constraints of the receiver FOV.

While we expect that the optimal FOV for the tracking receiver will be somewhere around the minimum FOV ($\chi_{min}$) that covers the whole light source when the receiver is flat and oriented upwards to face the transmitter, having different elevation angles to track the source causes the FOV to vary around $\chi_{min}$. This is why we use this optimization problem to get the optimal FOV per location and orientation for a specified source for maximum SNR. It is also useful for receivers that do not know the size of the sources and cannot measure the minimum FOV geometrically when the transmitters are non-circular which is fairly common.

Instead of optimizing continuously for the best FOV, we show results in section IV where fixing the FOV to the maximum FOV obtained from the optimization problem over a number of locations will give almost the same result as constantly evaluating the FOV from optimization problem. We also show that fixing the FOV to an inaccurate number may cause significant losses.

For comparison, we also analyze the D-FOV receiver without tracking [10]; it solves the following optimization problem;

$$\begin{aligned} \max_{j=1,\ldots,S} \quad & \max_{\chi} \mathsf{SNR_j}(\chi) \\ \text{s.t.} \quad & 0 \le \chi \le \chi_{\max} \end{aligned}$$

where $S$ is the total number of sources in the room. This receiver finds the best transmitter and FOV to get the highest SNR for a certain location and orientation. Derivation of this optimization is reported in [10].

## IV. Simulation Results

Our test configuration for simulation matches our physical testbed. The testbed consists of a $3 \times 5$ grid of off-the-shelf CREE luminaires (#CR22-32L-35K-S) with dimensions of

TABLE I: Simulation Parameters

| Parameter | Parameter Description | Value |
|---|---|---|
| $m$ | Lambertian order | 0.88 |
| B | Bandwidth | $5 \times 10^7$ Hz |
| A | Receiver area | $785 \times 10^{-9}$ m$^2$ |
| $\chi_{min}$ | Minimum FOV | 7.56° |
| $\chi_{max}$ | Maximum FOV | 40° |
| $P_t$ | Transmitted power | 1.4 W |
| $w$ | $T_x$ Element grid width | 15 |
| $n$ | $T_x$ Element grid length | 10 |
| $R$ | Responsivity | 28 |
| $h$ | Vertical height between Tx and Rx | 1.96 m |
| $i_d^2$ | Dark current noise | $68 \times 10^{-20}$ A$^2$ |
| $P_{txDC}$ | Noise DC power | 0.0022 V |

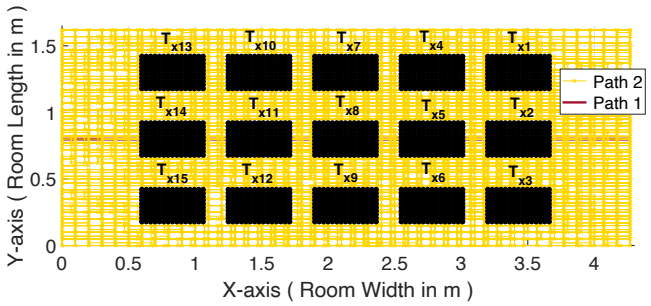


Fig. 2: Transmitter Setup

46 cm × 24 cm. The grid dimensions are 427 cm × 162 cm (x × y). The luminaires are positioned from the center with increments of 0.65 m in the x-axis and 0.5 m in the y-axis at a height of 2.68 m from the floor.

We apply our test configuration to the proposed system model to allow subsequent comparison of results against the real system implementation. However, as mentioned earlier, the system model is fully parameterized, permitting a wide range of room configurations to be studied. Simulation parameters measured in our lab are captured in Table I.

### A. Comparison Metrics

We use average SNR and number of handovers (HOs) as metrics used to compare performance of different receiver types. In terms of handover behavior, we study two different existing handover techniques [3]:

- MAX policy: The receiver finds the highest SNR received at its present location. This is characterized as following the envelope of the peak SNR at any point.
- HOLD policy: The receiver begins with the highest SNR on entering the space and holds this connection until the signal received drops below the threshold predefined by the user, at which point the receiver switches to the next maximum signal based on its present location. [1]

The transmitter setup is shown in Fig. 2. Two paths are highlighted within this figure; Path 1 crosses the room at a fixed location in the y-axis of the room and Path 2 is a random walk comprised of 50,000 steps within the room. Results from Path 1 help in easily visualizing the receiver performances while Path 2 gives more statistically useful results.

[1]Applying HOLD policy to the D-FOV non-tracking receiver changes its optimization problem, making it non-optimal in terms of average maximum SNR.

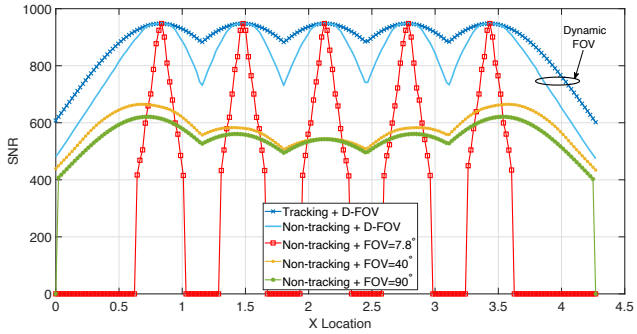


Fig. 3: Different Receiver Performance Under Path 1 with MAX Policy

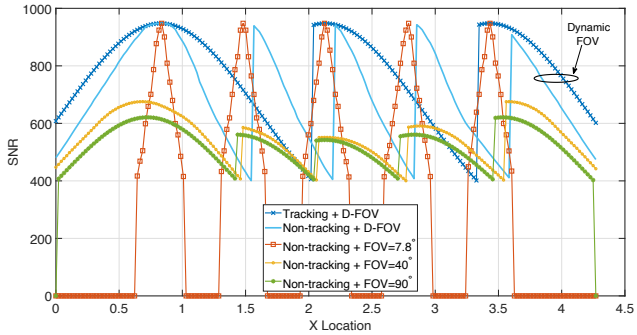


Fig. 4: Different Receiver Performance Under Path 1 HOLD Policy for $\beta = 400$

Fig. 3 shows how the different receiver setups perform when a user walks within the room on Path 1 (illustrated in Fig. 2) under MAX policy. We compare the performance of the D-FOV receiver in both cases tracking and non-tracking versus fixed FOV non-tracking receivers for different angles within our lab, $\chi = 7.84°$ which is the maximum FOV from our optimization, $\chi_{max} = 40°$ and a standard wide FOV (90°). The figure shows that the tracking D-FOV outperforms the non-tracking D-FOV receiver in the average SNR criteria but the price paid, due to MAX policy, is additional handovers (in comparison to other policies, i.e., HOLD). Still they are both superior to the other non-tracking fixed FOV receivers. Even though the non-tracking receiver with FOV fixed at 7.8° reaches high SNR values, it still lacks consistent coverage in many areas as shown in Fig. 3 and evaluated in Table III.

For the HOLD handover policy, Fig. 4 shows receiver performance on Path 1 at $\beta = 400$. It is clear that the dynamic FOV receivers generally outperform the static FOV receivers. The results also show that the tracking D-FOV receiver outperforms all other receivers in both metrics for

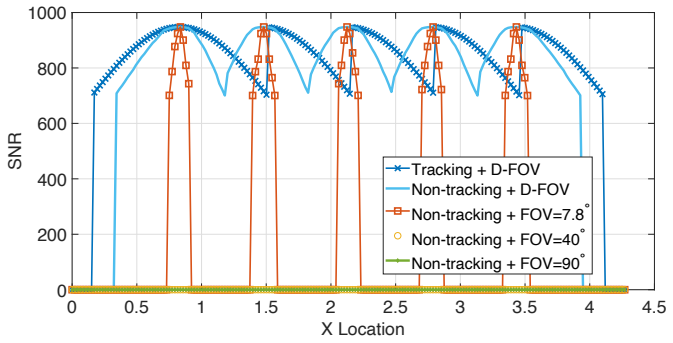


Fig. 5: Different Receiver Performance Under Path 1 for $\beta = 700$ with HOLD Policy

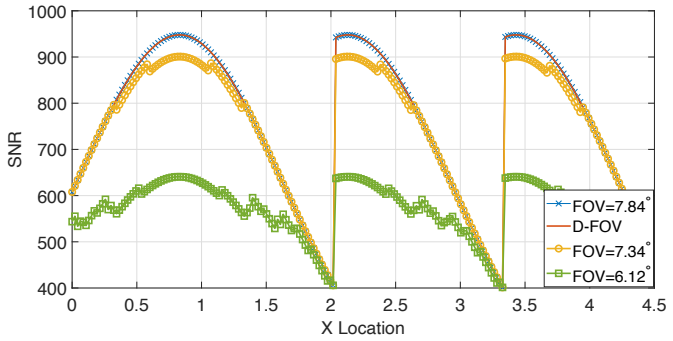


Fig. 6: Angle Sensitivity Effects on Tracking Receiver Performance (Path 1)

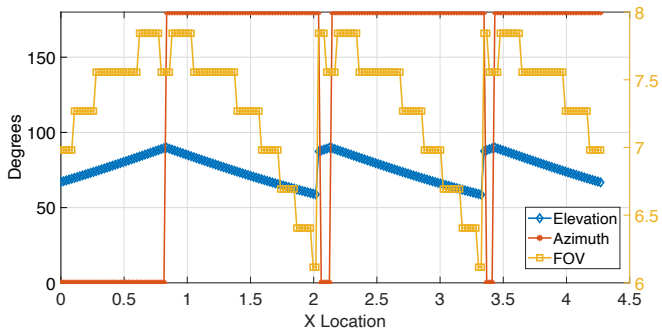


Fig. 7: Optimized Angles (Path 1)

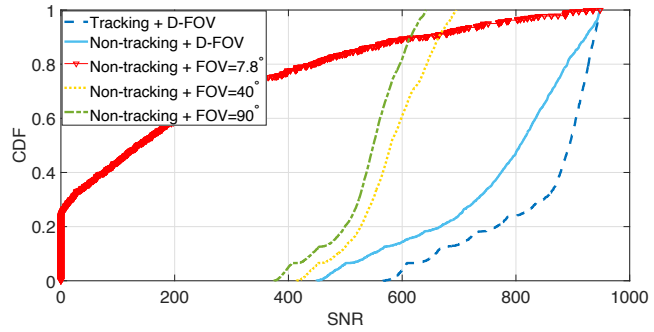


Fig. 8: SNR CDF (Path 2)

both policies. Values are summarized in Table III.

Note that $\beta$ plays an important role in the results shown. If we change its value to 700, the results in Fig. 5 show that Tracking D-FOV receiver approaches the performance of the non-tracking D-FOV receiver in number of Handovers (HOs) and the average max SNR is also close with an edge to the tracking receiver of the two under HOLD policy, (Table III).

The results in tables II, III and IV confirm that for the tracking receiver, if the FOV is fixed at the maximum from the optimization result ($7.84°$ in this scenario, not to be confused with $\chi_{max}$ which is defined in section III), we realize identical performance, mainly because the noise pattern does not change significantly at that FOV level. As the FOV increases more than $7.84°$, the SNR decreases. To be able to get the required FOV, the receiver can either keep solving the optimization problem until it goes underneath a light and then use the maximum FOV reached or if it knows the light source size and the source is circular it can use $\chi_{min}$ directly, however this is a sensitive number as the FOV does not change substantially; but the SNR can differ drastically as shown in Fig. 6. Note that for a rectangular source as in our model, setting the FOV fixed at $\chi_{min}$, yields a lower average max SNR, see Table II.

Fig. 6 shows results for the minimum FOV reached by the optimization including the maximum and the mean. Table II shows the average maximum SNR for each FOV. From the table we can see that within less than $2°$ difference, the average max SNR dropped by 196. This confirms how sensitive SNR is to get the optimal FOV for the best performance.

Fig.7 shows the changes in the optimized FOV[2] and the optimized $\theta_{elev}$ and $\theta_{az}$ from the tracking phase. While $\theta_{elev}$ is changing a lot, $\theta_{az}$ in this scenario it is either $0°$ or $180°$ because Path 1 is walking in a line under the lights.

Finally, Table IV shows the results for a more general random walk path (Path 2) which confirms the results previously discussed. The benefits of the tracking D-FOV receiver are clear in the reduction in number of handovers and high average SNR. Fig. 8 shows the SNR statistics, in terms of its cumulative distribution function (CDF), for the random walk path under MAX policy and confirms the benefits provided by the dynamic FOV receivers in comparison with the three fixed FOV receivers held at $7.8°$, $40°$ and the basic $90°$. This figure also shows how the smallest FOV suffers from coverage holes (SNR=0) but manages to catch up with the high SNR curves (Dynamic FOV receivers) in areas that are exactly under the lights.

[2]The dip in the FOV underneath the transmitters is attributed to the optimization problem as it seeks the minimum FOV to achieve the highest SNR although at these points slightly higher FOVs achieve the same SNR as well.

TABLE II: Average Max SNR for Tracking for Fixed FOVs

| Average max SNR | FOV (°) |
|---|---|
| 769.38 | 7.84° |
| 764.97 | $\chi_{min}$ |
| 751.35 | 7.34° |
| 572.98 | 6.12° |
| 769.38 | dynamic |

TABLE III: Path 1 Statistics

| | | Average max SNR | | HOs | | |
|---|---|---|---|---|---|---|
| HO policy | Tracking Status | $\beta = 400$ | $\beta = 700$ | $\beta = 400$ | $\beta = 700$ | FOV (°) |
| Hold | Tracking | 769.38 | 787.6 | 3 | 5 | dynamic |
| Hold | Non-tracking | 689.6 | 727.97 | 5 | 5 | dynamic |
| Hold | Non-tracking | 297.7 | 174.3 | 5 | 5 | 7.84° |
| Hold | Non-tracking | 550.5 | 0 | 5 | NA | 40° |
| Hold | Non-tracking | 518.95 | 0 | 5 | NA | 90° |
| Hold | Tracking | 769.37 | 787.6 | 3 | 5 | 7.84° |
| Max | Tracking | 882.7 | 882.7 | 5 | 5 | dynamic |
| Max | Non-tracking | 822.3 | 822.3 | 5 | 5 | dynamic |
| Max | Non-tracking | 381.7 | 381.7 | 5 | 5 | 7.84° |
| Max | Non-tracking | 585.5 | 585.5 | 5 | 5 | 40° |
| Max | Non-tracking | 546.4 | 546.4 | 5 | 5 | 90° |

### *B. Receiver Comparison*

While it makes sense to use the tracking D-FOV receiver based on its performance results, it is important to keep in mind that it is the most complex of the other receivers, as it needs to optimize $\chi$, $\theta_{Az}$ and $\theta_{elev}$. A good compromise is the tracking receiver with fixed FOV which is a variation of the previous receiver. Once the best FOV from the optimization is applied, we realize the same performance but without the need to recalculate $\chi$, for a fixed receiver height. Next in terms of complexity is the D-FOV receiver without tracking which optimizes $\chi$ to give high SNR.

The lowest-performing receiver is the one with fixed $\chi$ and fixed orientation because while it is the least complex one, based on the fixed FOV $\chi$, it sacrifices coverage or SNR. The smaller the FOV, the higher SNR per location and the more coverage holes occur, and vice versa.

TABLE IV: Path 2 Statistics at $\beta = 400$

| HO policy | Tracking Status | Average max SNR | HOs | FOV (°) |
|---|---|---|---|---|
| Hold | Tracking | 746.3 | 110 | dynamic |
| Hold | Non-tracking | 703.9 | 300 | dynamic |
| Hold | Non-tracking | 139.4 | 5477 | 7.84° |
| Hold | Non-tracking | 556.3 | 422 | 40° |
| Hold | Non-tracking | 505.96 | 1773 | 90° |
| Hold | Tracking | 746.3 | 110 | 7.84° |
| Max | Tracking | 861.69 | 3626 | dynamic |
| Max | Non-tracking | 773.9 | 4019 | dynamic |
| Max | Non-tracking | 139.4 | 4732 | 7.84° |
| Max | Non-tracking | 579 | 4019 | 40° |
| Max | Non-tracking | 521.9 | 4019 | 90° |

## V. Conclusion

Dense wireless networks promise to provide high speed links to a growing number of proximal user devices. Key to their success is the ability to isolate signals and avoid congestion typical of shared medium access. For optical networks, this isolation can be provided by controlling the receiver's orientation and FOV. In this paper we show how dynamic control of FOV and orientation has a significant impact on SNR at the receiver, enabling handover to exploit the availability of a best link. Performance analysis and simulation indicates the potential for this solution, with demonstrated gains of up to 40% in average maximum SNR over benchmark receivers with fixed orientation or with static FOV configurations.


## Acknowledgement

The authors would like to thank Islam El Bakoury for his valuable insight.


## References


[1] M. B. Rahaim, J. Morrison, and T. D. C. Little, "Beam control for indoor FSO and dynamic dual-use VLC lighting systems," *Journal of Communications and Information Networks*, vol. 2, no. 4, pp. 11–27, Dec 2017. [Online]. Available: https://doi.org/10.1007/s41650-017-0041-7

[2] T. D. C. Little, M. B. Rahaim, I. Abdalla, E. W. Lam, R. Mcallister, and A. M. Vegni, "A multi-cell lighting testbed for VLC and VLP," in *2018 Global LIFI Congress (GLC)*, Feb 2018, pp. 1–6.

[3] I. Abdalla, M. B. Rahaim, and T. D. C. Little, "Impact of receiver FOV and orientation on dense optical networks," in *Proc. GLOBECOMM 2018*, pp. 1–6.

[4] C. L. Bas, S. Sahuguede, A. Julien-Vergonjanne, A. Behlouli, P. Combeau, and L. Aveneau, "Impact of receiver orientation and position on visible light communication link performance," in *2015 4th International Workshop on Optical Wireless Communications (IWOW)*, Sept 2015, pp. 1–5.

[5] D. Ganti, W. Zhang, and M. Kavehrad, "VLC-based indoor positioning system with tracking capability using kalman and particle filters," in *2014 IEEE International Conference on Consumer Electronics (ICCE)*, Jan 2014, pp. 476–477.

[6] Y. S. Eroglu, I. Guvenc, N. Pala, and M. Yuksel, "AOA-based localization and tracking in multi-element VLC systems," in *2015 IEEE 16th Annual Wireless and Microwave Technology Conference (WAMICON)*, April 2015, pp. 1–5.

[7] Y. Kim, J. Hwang, J. Lee, and M. Yoo, "Position estimation algorithm based on tracking of received light intensity for indoor visible light communication systems," in *2011 Third International Conference on Ubiquitous and Future Networks (ICUFN)*, June 2011, pp. 131–134.

[8] S. Sheoran, P. Garg, and P. K. Sharma, "Location tracking for indoor VLC systems using intelligent photodiode receiver," *IET Communications*, vol. 12, no. 13, pp. 1589–1594, 2018.

[9] J. M. Kahn and J. R. Barry, "Wireless infrared communications," *Proceedings of the IEEE*, vol. 85, no. 2, pp. 265–298, Feb 1997.

[10] I. Abdalla, M. B. Rahaim, and T. D. C. Little, "Dynamic FOV visible light communications receiver for dense optical networks," *IET Communications*, February 2019.

[11] R. Ramirez-Iniguez, S. Idrus, and Z. Sun, "Optical wireless communications," *New York: Auerbach Publications*, 2008.

[12] T. Komine and M. Nakagawa, "Fundamental analysis for visible-light communication system using LED lights," *IEEE Transactions on Consumer Electronics*, vol. 50, no. 1, pp. 100–107, Feb 2004.